Theory of the structural phase transition in $A15$ compounds

Mitsuo Kataoka
The Research Institute for Iron, Steel and Other Metals, Tohoku University, Sendai 980, Japan
(Received 7 June 1982; revised manuscript received 2 December 1982)

The structural phase transition in the $A15$ compounds are investigated theoretically with the standpoint that the band Jahn-Teller effect of the twofold-degenerate Γ_{12} subbands crossing the Fermi level is responsible for the instability. On the basis of $\vec{k}\cdot\vec{p}$ perturbation theory, the Γ_{12} subbands are revealed to be well described by two parabolic bands which couple not only to the bulk distortions, but also to the displacements of the Γ_{12} optic modes. It is found that when the electron-lattice coupling exceeds the threshold of strength, the tetragonal phase with almost the same stabilities of $c/a>1$ and $c/a<1$ appears, accompanying one of the Γ_{12} optic modes below a weak first-order phase transition temperature T_M. The temperature dependences of the elastic moduli are calculated; it is found that $c_{11}-c_{12}$ vanishes below T_M while $c_{33}-c_{13}$ recovers from its softening partially or completely with decreasing temperature below T_M. The long-wavelength acoustic phonons are also investigated in order to clarify the relation between the phonon anomalies and the structural transition. The $[110]T_1$ mode ($\vec{q}||[110]$, $\vec{e}||[1\bar{1}0]$) is considerably softened in the range $0<q\lesssim 2k_F$. This softening begins at high temperatures, remaining even at absolute zero. The theory explains successfully the various aspects of the phase transitions in V_3Si and Nb_3Sn. The comparison between them proves that *the second-order Jahn-Teller effect* occurs in both compounds.

I. INTRODUCTION

Some of the $A15$ compounds are of interest because of their high-temperature superconductivity and their structural phase transition. A strong correlation between the two phase transitions is implied by the experimental fact that compounds with a high superconducting transition temperature T_c have large anomalies in the structural and electrical properties. Although much effort has been devoted to the subject, the microscopic origins of the superconducting and structural anomalies have not been fully clarified. Most of the earlier works were reviewed by some authors.[1–3] The purpose of this paper is to investigate theoretically the structural phase transition by developing the theory recently proposed by the author.[4]

V_3Si and Nb_3Sn undergo the martensitic cubic-to-tetragonal transition at $T_M\simeq 21$ and 43 K, respectively. Some experiments show that the phase transitions are nearly of second order in contrast to the usual martensitic transitions. In the low-temperature phase, $c/a>1$ in V_3Si (Ref. 5) and $c/a<1$ in Nb_3Sn.[6] According to the neutron-diffraction experiments,[7] the internal relative displacements with the Γ_{12} symmetry are superposed on the uniform tetragonal distortion. The two kinds of displacement have almost the same temperature dependence. When Nb_3Sn is doped with Al or Sb, the tetragonal distortion switches from $c/a<1$ to $c/a>1$ at some concentrations, while the magnitude of the distortion does not change significantly.[8,9] This shows comparable stabilities of the two phases with $c/a<1$ and $c/a>1$. One of the precursor effects of the structural transition is the softening of $c_{11}-c_{12}$ in the cubic phase. With decreasing temperature, $c_{11}-c_{12}$ decreases and almost vanishes at the almost second-order transition temperature T_M. However, $c_{11}-c_{12}$ does not recover from its softening in the low-temperature phase.[10,11] This behavior of the softening is quite different from those observed for many other structural phase transitions. Shirane, Axe, and also Birgeneau carried the experiments of neutron inelastic scattering on Nb_3Sn and V_3Si, and observed the softening of the long-wavelength acoustic phonons.[12–14] The softening of the $[110]T_1$ mode is most remarkable and is spread out in a wide range of the reciprocal space. Moreover, this softening is strongly dependent on temperature. The [110]L mode, on the other hand, shows a small softening and a weak temperature dependence. The Γ_{12} optic-phonon modes in V_3Si were investigated by Raman scattering experiments.[15] Their frequencies have only a weak tem-

perature dependence above T_M, though the Γ_{12} modes definitely contribute to the structural phase transition.[7] It should be noted that in spite of the different signs of the tetragonal distortions in V_3Si and Nb_3Sn, some of the above peculiar properties are common to both compounds.

Among the theories of the origin of the structural transition in $A15$ compounds, the two proposed by Labbé and Friedel[16] and by Gor'kov[17] were developed by many authors to obtain better agreements between the theory and experiments. A feature common to the theories is the stabilization of the tetragonal phase by lifting degeneracies of electronic bands near the Fermi energy ϵ_F, i.e., the stabilization through the band Jahn-Teller effect. Labbé and Friedel assumed three independent one-dimensional bands consisting of d orbitals on the transition-metal cations lined up along the three directions parallel to the cubic axes. The degeneracy of the bottoms of the assumed bands is lifted by a change of the bandwidths due to the tetragonal distortion; if ϵ_F is nearly adjacent to the band bottoms in the cubic phase, the electronic energy is lowered by redistributing electrons to the split bands. Gor'kov[17] and Gor'kov and Dorokhov,[18] on the other hand, asserted that band degeneracies at the X points owing to the nonsymmorphic crystal structure of $A15$ are important to the structural instability. Also in this model one dimensionality was assumed so that the Fermi surface has well-developed flat portions containing the X points. However, the band structures assumed by them are inconsistent with the results of the augmented-plane-wave (APW) band calculations.[19,20] In fact, neither theory can explain the almost second-order phase transition and/or $c_{11}-c_{12}\simeq 0$ in the low-temperature phase, although some of the other aspects of the phase transition are explained successfully.

Klein, Boyer, Papaconstantopoulos, and Mattheiss[20] performed the self-consistent APW band calculations for $A15$ compounds. Their result shows that some $A15$ compounds including V_3Si and Nb_3Sn possess two very flat bands evolving from the Γ_{12} doublet states near ϵ_F. The similar band structures were also obtained by using the self-consistent pseudopotential method[21] and the linear-muffin-tin orbital method.[22] Recently, the author showed on the basis of $\vec{k}\cdot\vec{p}$ perturbation theory that the Γ_{12} subbands are split by the tetragonal distortion and are responsible for the structural transition.[4] In the present paper we develop the theory as follows:

(i) Two parabolic bands instead of the bands with a constant density of states are used for the Γ_{12} subbands. $\vec{k}\cdot\vec{p}$ perturbation theory proves that the parabolic bands give the true Γ_{12} subbands in a small region containing the Γ point. In the case of a weak electron-lattice coupling, this alteration is essential in determining the equilibrium state.

(ii) Γ_{12} optic modes are taken into consideration. These modes can couple not only to the bulk distortions but also to the Γ_{12} electronic subbands, and therefore contribute to the structural transition.

(iii) The dynamics of this electron-lattice system are also investigated in order to clarify the relation between the phonon anomalies and the structural transition.

Sham[23] and Noolandi and Sham[24] discussed the optic modes and the lattice dynamics on the assumption that threefold-degenerate one-dimensional bands cause the structural instability. Bhatt and McMillan[25] also discussed them on the basis of the Gor'kov model. Making arguments parallel to the above-mentioned works for the case of the Γ_{12} subbands, we see in the following sections that the Γ_{12}-subband model can explain various aspects of the observed structural transitions.

In the next section the bulk distortions, optic displacement modes, and electronic states with Γ_{12} symmetry are introduced. The Γ_{12} subbands in the presence of both kinds of ionic displacement are obtained by using $\vec{k}\cdot\vec{p}$ perturbation theory. In Sec. III we derive the free energy of the electron-lattice system, discussing the condition for the structural instability, equilibrium distortion, and the properties of the phase transition. In Sec. IV the isothermal elastic constants are calculated and compared to the experimental data on V_3Si and Nb_3Sn. Section V is devoted for the investigation of the dynamics of the electron-lattice system. The self-consistent equations for the motions of electrons and ions are obtained by using the linear-response theory, and are solved to find the phonon softening. Finally (in Sec. VI), concluding remarks are given.

II. Γ_{12} SUBBANDS IN THE PRESENCE OF IONIC DISPLACEMENTS

Figure 1 shows the unit cell of A_3B with the $A15$ structure whose space group is $Pm3n$ (O_h^3). The unit cell contains two molecules. The six A sites, which are occupied usually by transition-metal cations, are numbered as shown in Fig. 1. Since the symmetric representation of Γ_{12}, $[\Gamma_{12}\times\Gamma_{12}]$, is decomposed into the representations Γ_1 and Γ_{12}, Γ_{12} electronic states couple to the Γ_1 and Γ_{12} modes of ionic displacement. The Γ_1 mode corresponds to a volume change and does not play an important role in the structural change. The bulk distortion with the Γ_{12} symmetry is given by

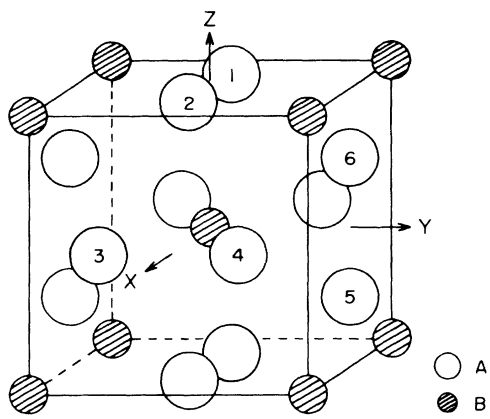

FIG. 1. Unit cell of the A_3B compounds with the A 15 structure. The space group is $Pm3n$ (O_h^3). The B sites form a bcc lattice and the A sites form three orthogonal chains along the cube faces. The unit cell contains two molecules. The A sites are numbered as shown.

$$u_2=(e_{xx}-e_{yy})/\sqrt{2}\ ,\qquad u_3=(2e_{zz}-e_{xx}-e_{yy})/\sqrt{6}\ , \tag{1}$$

where e_{xx}, etc., are the strain components. In addition to the bulk distortions, the $A15$ structure has the internal relative displacements with the Γ_{12} symmetry, i.e., the Γ_{12} optic modes, which are expressed by a general form as

$$Q_s=\sum_{\kappa,i}\sqrt{Nm_\kappa}\,e_{\kappa i,s}u_{\kappa i}\ , \tag{2}$$

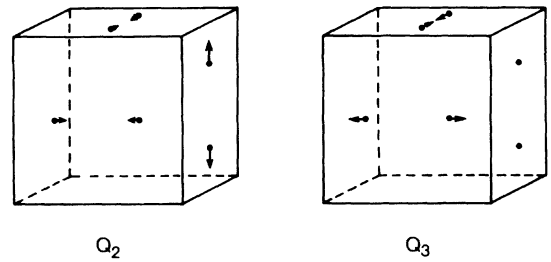

FIG. 2. Ionic displacements of the Γ_{12} optic modes Q_2 and Q_3. Only A ions are displaced along the A-ion chain directions. It is noted that Q_2 and Q_3 are transformed as u_2 and u_3, respectively, by the crystal symmetry operations.

where $s=2$ or 3, N is the total number of unit cells, $u_{\kappa i}$ is the ith component of the displacement vector of the κth ion in a unit cell, $e_{\kappa i,s}$ is the κi component of the eigenvector of the normal mode s, and m_κ is the κth ion's mass. A group-theoretical argument proves that

$$\begin{aligned}Q_2&=\sqrt{Nm_A}(2u_{6z}-2u_{5z}-u_{2x}+u_{1x}-u_{4y}+u_{3y})/2\sqrt{3}\ ,\\ Q_3&=\sqrt{Nm_A}(-u_{2x}+u_{1x}+u_{4y}-u_{3y})/2\ ,\end{aligned} \tag{3}$$

where m_A is the A ion's mass.[23] The ionic displacements expressed by Q_2 and Q_3 are shown in Fig. 2. On the other hand, Γ_{12} electronic states in the absence of the ionic displacements are written as follows:

$$\begin{aligned}
&\Psi_\nu=b_d\psi_{d\nu}+b_d'\psi_{d\nu}'+b_p\psi_{p\nu},\quad \nu=2,3\\
&\psi_{d2}=(d_{1,3x^2-r^2}+d_{2,3x^2-r^2}-d_{3,3y^2-r^2}-d_{4,3y^2-r^2})/2\ ,\\
&\psi_{d3}=(2d_{5,3z^2-r^2}+2d_{6,3z^2-r^2}-d_{1,3x^2-r^2}-d_{2,3x^2-r^2}-d_{3,3y^2-r^2}-d_{4,3y^2-r^2})/2\sqrt{3}\ ,\\
&\psi_{d2}'=(2d_{5,x^2-y^2}+2d_{6,x^2-y^2}-d_{1,y^2-z^2}-d_{2,y^2-z^2}-d_{3,z^2-x^2}-d_{4,z^2-x^2})/2\sqrt{3}\ ,\\
&\psi_{d3}'=(-d_{1,y^2-z^2}-d_{2,y^2-z^2}+d_{3,z^2-x^2}+d_{4,z^2-x^2})/2\ ,\\
&\psi_{p2}=(2p_{6,z}-2p_{5,z}-p_{2,x}+p_{1,x}-p_{4,y}+p_{3,y})/2\sqrt{3}\ ,\\
&\psi_{p3}=(p_{2,x}-p_{1,x}-p_{4,y}+p_{3,y})/2\ ,
\end{aligned} \tag{4}$$

where the functions d_κ and p_κ are the valence d and p orbitals on the κth ion, respectively, and the quantities b represent magnitudes of hybridizations between these orbitals. It is noted that orbitals on the B ions cannot be hybridized with Ψ_2 and Ψ_3. The results of the APW band calculations[20] show that the quantities b have comparable orders of magnitude. The orbitals d_{1,y^2-z^2}, etc., have their large densities in planes perpendicular to the directions of the A-ion chains, while $d_{1,3x^2-r^2}$, etc., and $p_{1,x}$, etc., have their large densities in the chain's directions. The latter two kinds of orbital, therefore, couple strongly to the displacements given by Eqs. (1) and (3), playing an important role in the structural transition.[26,27]

The Γ_{12} subbands in a small region containing the Γ point in the presence of the ionic displacements with the Γ_{12} symmetry are known by $\vec{k}\cdot\vec{p}$ perturbation theory.[4,28] The effective Hamiltonian $H_{\vec{k}}$ for the band states with wave vector $\vec{k}$ has been shown to be given by

$$H_{\vec{k}}=\frac{\hbar^2k^2}{2m^*}(a_2^\dagger a_2+a_3^\dagger a_3)+\left\{\left[\left[\frac{c_0V}{N}\right]^{1/2}g_0u_2+\frac{\omega_i}{\sqrt{N}}g_iQ_2\right]+\frac{\hbar^2}{2m_a^*}\frac{1}{\sqrt{2}}(k_x^2-k_y^2)\right\}(a_2^\dagger a_3+a_3^\dagger a_2)$$

$$+\left\{\left[\left[\frac{c_0V}{N}\right]^{1/2}g_0u_3+\frac{\omega_i}{\sqrt{N}}g_iQ_3\right]+\frac{\hbar^2}{2m_a^*}\frac{1}{\sqrt{6}}(3k_z^2-k^2)\right\}(a_2^\dagger a_2-a_3^\dagger a_3)\ , \tag{5}$$

where a_ν and $a_\nu^\dagger$ are, respectively, the annihilation and creation operators of electrons in Ψ_ν, m^* and m_a^* are, respectively, the isotropic and anisotropic effective masses, g_0 is the coupling constant between the electron and the uniform distortions while g_i is the coupling constant between the electron and the internal relative displacements, c_0 $(\equiv c_{11}^0-c_{12}^0)$ is an elastic constant in the absence of the Γ_{12} electron-lattice coupling, V is the crystal volume, and ω_i is the frequency of the Γ_{12} optic modes. The terms in $\hbar^2/2m_a^*$ in Eq. (5) arise from the mixing of the Γ_{12} states and the other bands. The band-structure calculations show that the Γ_{12} states are isolated far from the other bands near the Γ point. Therefore the terms in $\hbar^2/2m_a^*$ are small compared to the terms in $\hbar^2/2m^*$ and are neglected for simplicity in the following. Since the difference between m^* and the bare free-electron mass m arises also from the band mixing, the Γ_{12} subbands in the absence of the ionic displacements become twofold-degenerate parabolic bands with the effective mass comparable to the bare electron mass. We transform a_ν into $a_{\vec{k}\nu}$ by

$$a_{\vec{k}\nu}=\sum_{\nu'=2}^{3}U_{\nu\nu'}^e a_{\nu'}\ , \tag{6}$$

where

$$U_{22}^e=U_{33}^e=\cos(\theta/2)\ ,\qquad U_{23}^e=-U_{32}^e=\sin(\theta/2)\ , \tag{7}$$

with

$$\theta=\tan^{-1}\left[\frac{\sqrt{c_0V}g_0u_2+\omega_ig_iQ_2}{\sqrt{c_0V}g_0u_3+\omega_ig_iQ_3}\right]\ . \tag{8}$$

Then $H_{\vec{k}}$ is diagonalized as follows:

$$H_{\vec{k}}=\epsilon_{\vec{k}2}a_{\vec{k}2}^\dagger a_{\vec{k}2}+\epsilon_{\vec{k}3}a_{\vec{k}3}^\dagger a_{\vec{k}3}\ , \tag{9}$$

$$\left.\begin{matrix}\epsilon_{\vec{k}2}\\ \epsilon_{\vec{k}3}\end{matrix}\right\}=\frac{\hbar^2k^2}{2m^*}\pm\left\{\left[\left[\frac{c_0V}{N}\right]^{1/2}g_0u_2+\frac{\omega_i}{\sqrt{N}}g_iQ_2\right]^2+\left[\left[\frac{c_0V}{N}\right]^{1/2}g_0u_3+\frac{\omega_i}{\sqrt{N}}g_iQ_3\right]^2\right\}^{1/2}\ . \tag{10}$$

The obtained bands (10) with no ionic displacements show some of the properties of the Γ_{12} subbands calculated by the APW method, such as their large positive effective mass and the fairly isotropic nature around the Γ point. The deviations between the parabolic bands and the true bands increase with increasing k. Without going into more detail of the true band structure, we study the structural transition on the basis of the bands (10) by assuming that the deviations do not change the qualitative properties of the structural transition when the Fermi momentum is sufficiently small and k_BT_M is much smaller than the bandwidths. It should be noted that the electron-lattice coupling in Eq. (10) is very different from those in the other band models.[16,17,24,25]

III. EQUILIBRIUM DISPLACEMENTS IN THE LOW-TEMPERATURE PHASE

The Fermi level ϵ_F crosses not only the Γ_{12} subbands, but also some other bands consisting of s orbitals of A ions and p orbitals of B ions.[20] The latter bands have only small densities of states at ϵ_F and are insensitive to the diplacements given by Eqs. (1) and (3). Assuming that the effects of these bands are included in the lattice free energy, we consider the only Γ_{12} subbands explicitly for the electronic free energy. The total free energy of the electron-lattice system is then given by

$$F=\tfrac{1}{2}Vc_0(u_2^2+u_3^2)+\tfrac{1}{2}\omega_i^2(Q_2^2+Q_3^2)+\zeta\sqrt{Vc_0}\omega_i(u_2Q_2+u_3Q_3)+Vn\mu$$
$$-2k_BT\sum_{\vec{k}}(\ln\{1+\exp[-(\epsilon_{\vec{k}2}-\mu)/k_BT]\}+\ln\{1+\exp[-(\epsilon_{\vec{k}3}-\mu)/k_BT]\}) , \quad (11)$$

where μ is the chemical potential, n is the number of electrons in the Γ_{12} subbands per unit volume, k_B is the Boltzmann constant, and T is temperature. The first and the second terms on the right-hand side of Eq. (11) are, respectively, the energies of the bulk distortions and the optic-mode displacements. The third term is the energy of the coupling between the two types of displacement[24,25] with the dimensionless coupling constant ζ. This term arises from the fact that the A sites are not at centers of symmetry.[29] The other terms are the electronic contribution to the free energy. The equilibrium displacements are obtained by minimizing the free energy (11) with respect to u_2, u_3, Q_2, Q_3, and also μ. We can easily prove that the equilibrium displacements have the relation

$$Q_\nu=\frac{\sqrt{c_0V}}{\omega_i}\left[\frac{g_i-\zeta g_0}{g_0-\zeta g_i}\right]u_\nu \quad (12)$$

at any temperature. The linear relation was obtained also for the other band models.[24,25] If higher-order terms in u_ν and Q_ν, which were not taken into consideration in Eq. (11) [see Eq. (17)], cannot be neglected, the linearity does not hold true. Substituting Eq. (12) into Eq. (11), we obtain the effective free energy as

$$F/V=\tfrac{1}{2}C_0u^2+\mu n-k_BT\int\mathscr{D}(\epsilon)(\ln\{1+\exp[-(\epsilon+\sqrt{C_0V/N}G_0u-\mu)/k_BT]\}$$
$$+\ln\{1+\exp[-(\epsilon-\sqrt{C_0V/N}G_0u-\mu)/k_BT]\})d\epsilon . \quad (13)$$

Here we used the definitions

$$u=(u_2^2+u_3^2)^{1/2} ,$$
$$C_0=c_0^e\left[1+\frac{(1-\zeta^2)g_i^2}{(g_0-\zeta g_i)^2}\right] ,$$
$$G_0=|g_0|\left[1+\frac{(g_i-\zeta g_0)^2}{(1-\zeta^2)g_0^2}\right]^{1/2} ,$$
$$\mathscr{D}(\epsilon)=(2\pi^2)^{-1}(2m^*/\hbar^2)^{3/2}\sqrt{\epsilon} ,$$

where

$$c_0^e=(1-\zeta^2)c_0 .$$

The quantity c_0^e is the effective elastic constant of u_2 and u_3 for a crystal without the Γ_{12} subbands, and should be positive to stabilize the crystal. The renormalized constants C_0 and G_0 always become larger than c_0^e and $|g_0|$ because the bulk distortions accompany the optic modes. Equation (13) gives the equilibrium conditions as follows:

$$u=\left[\frac{V}{NC_0}\right]^{1/2}G_0\int\mathscr{D}(\epsilon)[f_3(\epsilon)-f_2(\epsilon)]d\epsilon , \quad (14)$$

$$n=\int\mathscr{D}(\epsilon)[f_3(\epsilon)+f_2(\epsilon)]d\epsilon , \quad (15)$$

with

$$\left.\begin{matrix}f_2(\epsilon)\\ f_3(\epsilon)\end{matrix}\right\}=\{1+\exp[(\epsilon\pm\sqrt{C_0V/N}G_0u-\mu)/k_BT]\}^{-1} . \quad (16)$$

Equations (14)–(16) determine $u=(u_2^2+u_3^2)^{1/2}$ but not $u_2/u_3=\tan\theta$. The directions $\theta=0$, $2\pi/3$, and $4\pi/3$ correspond, respectively, to elongations along the z, x, and y axes, whereas the directions $\theta=\pi/3$, π, and $5\pi/3$ correspond, respectively, to contractions along the y, z, and x axes; the other general directions give orthorhombic distortions. In our simplified theory, these kinds of bulk distortion with a common u have the same stability. The reason for this isotropy in the u_2-u_3 plane is that the ground subband $\epsilon_{\vec{k}3}$ can be lowered by the same amount for any θ if $-\sin(\theta/2)\Psi_2+\cos(\theta/2)\Psi_3$ is chosen for the ground subband [see Eqs. (6)–(10)]. Such isotropic nature was not obtained for any other previous model of the structural transition in the $A15$ compounds. For real substances, however, there exist small anisotropy energies in the u_2-u_3 plane, which originate from some higher-order effects[30] and the band anisotropies. For our isotropic band model, the most important anisotropy energy F_3 is given by

$$F_3/V=(A_3-B_3)u^3\cos(3\theta) . \quad (17)$$

In Eq. (17) the term in A_3 is the anharmonic lattice energy; the term in B_3 arises from the electron-

lattice coupling which is quadratic in the displacements, as shown in Appendix A. The tetragonal distortion $c/a>1$ or $c/a<1$ is realized for a negative or positive constant (A_3-B_3), respectively. The magnitudes of the tetragonal distortions in V_3Si and Nb_3Sn are caused mainly by the linear coupling between the distortions and the Γ_{12}-subband electrons, but the signs $c/a-1>0$ in V_3Si and $c/a-1<0$ in Nb_3Sn are determined by the anisotropy energy. We suppose that for Nb_3Sn, the dopants Al and Sn change the sign of $c/a-1$ by changing the sign of A_3-B_3. This gives an explanation of the observed fact that the magnitude of the distortion does not change significantly in spite of the change of the sign of $c/a-1$ by the dopants.[8,9]

In the following we assume a tetragonal distortion $|u_3|=u$ and $u_2=0$ for the equilibrium state. The coupled equations (14) and (15) for u and μ are solved numerically. The equilibrium distortion u is proved to be characterized by only α, which is defined by

$$\alpha=2a_0^3\mathscr{D}(\epsilon_F)G_0^2 , \tag{18}$$

where a_0 is the lattice constant of the undistorted crystal. Figure 3 shows the equilibrium u and μ at zero temperature together with the transition temperature T_M as functions of α. The phase transition occurs only for $\alpha>1$. For $1<\alpha\leq\frac{3}{4}(4)^{1/3}$ ($\simeq 1.19$), both the upper and lower bands are partially occupied by electrons in the equilibrium state, i.e., the second-order Jahn-Teller effect works. For $\frac{3}{4}(4)^{1/3}<\alpha$, the upper band is completely empty, i.e., the first-order Jahn-Teller effect works. These situations are shown in Fig. 4. It is noted that the former case does not occur for the band structure with a constant density of states, which was assumed in Ref. 4. The two cases are expected to have strongly different properties of superconductivity, elasticity, etc. As will be shown in the following sections, α for Nb_3Sn is determined to be 1.08 by using the experimental data of the elastic constant and the acoustic-phonon frequency. Also for V_3Si, α can be expected to have a value near 1.08. The second-order Jahn-Teller effect, therefore, occurs in both compounds. This result is in accordance with the prediction made by Weger and Goldberg.[1]

The free energy (13) is an even function of u and gives the second-order phase transition irrespective of the value of α. The energy F_3 given by Eq. (17) always makes the transition to be of the first order.[30,31] The first-order phase transitions in V_3Si and Nb_3Sn were confirmed by the thermal-expansion[32] and x-ray-diffraction[33] measurements. However, many experimental data, such as those of x-ray diffraction,[5,6] magnetic susceptibility,[34,35] and elastic constant,[10,11] show that the transitions of these compounds are almost of the second order. From this experimental fact, the energy F_3 is found to be small enough to be neglected in the temperature dependences of u. In Fig. 5, the calculated u by use of Eqs. (14) and (15) is shown and is compared to the observed data on V_3Si and Nb_3Sn. As seen in Fig. 5, the calculated distortion decreases faster than the observed distortions with increasing temperature. This discrepancy arises from the experimental fact that the development of the tetragonal distortion is arrested in the superconducting phase. Shirane and Axe[7] observed the same temperature dependences of the tetragonal distortion and the

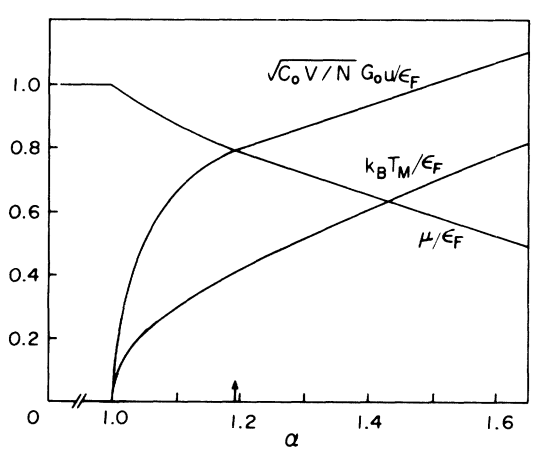

FIG. 3. Bulk distortion u and chemical potential μ at zero temperature together with phase-transition temperature T_M as functions of α. The phase transition occurs only when $1<\alpha$. The second-order Jahn-Teller effect works below the value of α indicated by the arrow in the figure, and the first-order Jahn-Teller effect works above the value of α. In the latter case, u and μ are linear in α.

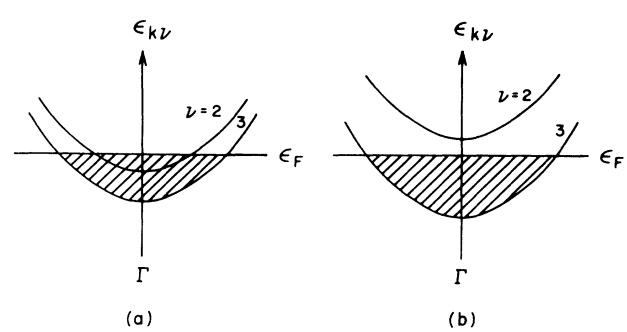

FIG. 4. Γ_{12} subbands affected by the band Jahn-Teller effect. (a) corresponds to the case of the second-order Jahn-Teller effect which works for $1<\alpha\leq\frac{3}{4}(4)^{1/3}$. (b) corresponds to the case of the first-order Jahn-Teller effect which works for $\frac{3}{4}(4)^{1/3}<\alpha$.

Γ_{12}—optic-mode displacement.[36] This also shows the smallness of F_3.

IV. ISOTHERMAL ELASTIC CONSTANTS

The elastic constants of the system consisting of the bulk distortions, the optic-mode displacements, and the band electrons are calculated by the same way as in Refs. 4 and 37. When the further distortions from the equilibrium state, δu_2 and δu_3, are induced by applying an external stress, they change the electron distribution, which induces further the optic-mode displacements. After the rearrangement of these internal variables, the free energy depends on only δu_2 and δu_3. The free energy of the tetragonal phase has the approximate form as

$$F = F_0 + \tfrac{1}{2} V(c_{11} - c_{12})(\delta u_2)^2 + \tfrac{1}{2} V(c_{33} - c_{13})(\delta u_3)^2 , \quad (19)$$

where F_0 is the free energy of the equilibrium state and the quantities c are the isothermal elastic constants affected by the electron-lattice coupling. Expanding F given by Eq. (11) in powers of not only δu_2 and δu_3 but also δQ_2 and δQ_3, which are the further displacements of the equilibrium Q_2 and Q_3, up to the second order, and minimizing this free energy with respect to δQ_2 and δQ_3, we arrive at the same form as Eq. (19). A comparison between this and Eq. (19) gives the elastic constants in the tetragonal phase as

$$c_{11} - c_{12} = 0 , \quad (20)$$

$$c_{33} - c_{13} = c_0^e \left[\frac{1 - \alpha X(T,u)}{1 - \Theta X(T,u)} \right] , \quad (21)$$

with

$$[X(T,u)]^{-1} = \tfrac{1}{2} k_B T \mathscr{D}(\epsilon_F) \left[\left[\int \mathscr{D}(\epsilon) f_2(\epsilon)[1 - f_2(\epsilon)] d\epsilon \right]^{-1} + \left[\int \mathscr{D}(\epsilon) f_3(\epsilon)[1 - f_3(\epsilon)] d\epsilon \right]^{-1} \right] , \quad (22)$$

where Θ represents a contribution of the Γ_{12} optic modes to α and is expressed by

$$\Theta = 2 a_0^3 \mathscr{D}(\epsilon_F) g_i^2 .$$

In obtaining Eqs. (20)–(22), we already used the equilibrium conditions (14) and (15) and also $c_{33} - c_{13} = 0$ at the transition temperature T_M; T_M satisfies

$$X(T_M, 0) = 1/\alpha . \quad (23)$$

The elastic constants in the cubic phase are obtained by taking account of $u_2 = u_3 = Q_2 = Q_3 = 0$ as

$$c_{11} - c_{12} = c_{33} - c_{13} = c_0^e \left[\frac{1 - \alpha X(T,0)}{1 - \Theta X(T,0)} \right] . \quad (24)$$

Expressions of the elastic constants similar to those given by Eqs. (21) and (24) were obtained for a localized electron system exhibiting the cooperative Jahn-Teller effect[37] and for the band-electron systems.[24,25] Equation (20) shows that $c_{11} - c_{12}$ vanishes below T_M even when δu_2 accompanies δQ_2. This anomalous behavior of $c_{11} - c_{12}$ originates from the isotropic nature of the electron-lattice coupling in Eq. (10) and of the free energy (13) in the u_2-u_3 plane, being characteristic of the Γ_{12}-subband model. In order to understand this result, we depict our free energies below and above T_M in Fig. 6. As seen from Fig. 6(a), the deviation δu_3 from an equilibrium tetragonal distortion increases the free energy, but δu_2 does not increase the free energy in the harmonic approximation. This is the reason for $c_{33} - c_{13} \neq 0$ and $c_{11} - c_{12} = 0$ below T_M. Above T_M, on the other hand, both δu_2 and δu_3 increase the free energy and $c_{11} - c_{12}$ $(= c_{33} - c_{13})$ has a nonzero value except at $T = T_M$. When the anisotropy energy (17) cannot be neglected, $c_{11} - c_{12}$ below T_M no longer vanishes. However, $c_{11} - c_{12}$ remains small for the small anisotropy energy. The electron-lattice couplings in the previous models do not have an iso-

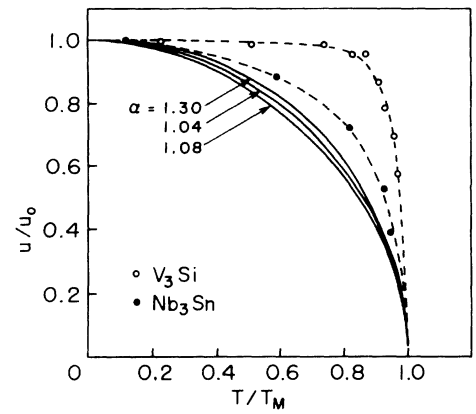

FIG. 5. Temperature dependence of the bulk distortion u. Solid lines are the calculations and the dashed lines are simple extrapolations of the experimental data on V_3Si (Ref. 5) and Nb_3Sn (Ref. 6). Both lines are depicted by normalizing distortions by those at zero temperature. The superconducting phase appears at $T/T_M \simeq 0.8$ in V_3Si and 0.4 in Nb_3Sn. The effect of the superconductivity on u is not taken into account in the calculations.

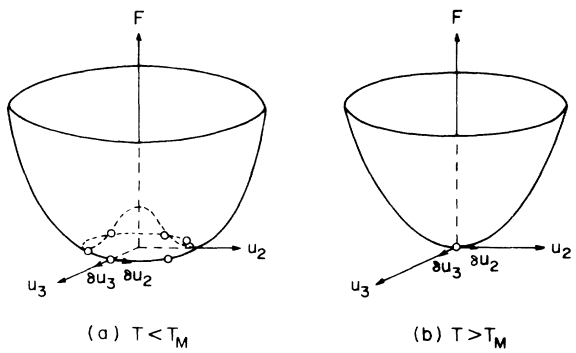

FIG. 6. Free energies below and above T_M. The circles ○ show the possible equilibrium points. At $T<T_M$, the tetragonal distortions with $c/a>1$ $[\theta=\tan^{-1}(u_2/u_3)=0,\pm 2\pi/3]$ or $c/a<1$ $(\theta=\pi,\pm\pi/3)$ are realized by the anisotropy energy F_3. If F_3 is sufficiently small, δu_2 does not give rise to a significant increase of the energy, in contrast to δu_3, in the low-temperature phase.

tropic nature as in the Γ_{12}-subband model. Therefore both $c_{11}-c_{12}$ and $c_{33}-c_{13}$ in those models recover from the softenings with decreasing T from T_M.[24,25]

The temperature dependences of the elastic constants depend on α and Θ. The calculated elastic constants are shown in Fig. 7 for some values of α and Θ/α. When α and Θ/α have small values, $c_{11}-c_{12}$ in the cubic phase is remarkably softened even at high temperatures and has an inflection point near T_M. In the tetragonal phase, the softening of $c_{33}-c_{13}$ decreases with decreasing T. At $T=0$, $c_{33}-c_{13}$ becomes c_0^e for $\alpha>\frac{3}{4}(4)^{1/3}$, while it is still softened for $1<\alpha<\frac{3}{4}(4)^{1/3}$. This is because in the latter case an electronic contribution to the elastic constants partially cancels c_0^e. Both $c_{11}-c_{12}$ in the cubic phase and $c_{33}-c_{13}$ rise more steeply for larger values of Θ/α with increasing $|T-T_M|$. Figure 7 also gives a comparison between the calculated curves and the experimental data on V_3Si (Ref. 10) and Nb_3Sn.[11] We obtained $\alpha=1.08$ and $\Theta=0.22$ for Nb_3Sn by fitting the calculated curves of $c_{11}-c_{12}$ and the phonon dispersions (see Sec. V) to the experimental data. The same temperature dependences of the observed elastic constants $c_{11}-c_{12}$ in Nb_3Sn and V_3Si show that V_3Si has similar values of α and Θ to those of Nb_3Sn. Agreement between the theory and the experiments is satisfactory.[38] From a small value of Θ/α we find that the Γ_{12} optic modes do not play a main role in the structural phase transition in these compounds. As shown in Fig. 7, the observed elastic constants $c_{11}-c_{12}$ of both compounds are very small below T_M in agreement with the calculation. This gives another confirmation of the smallness of the energy (17). Unfortunately, we have no experimental data of $c_{33}-c_{13}$ at present, which can distinguish the cases $1<\alpha<\frac{3}{4}(4)^{1/3}$ and $\frac{3}{4}(4)^{1/3}<\alpha$ most directly.

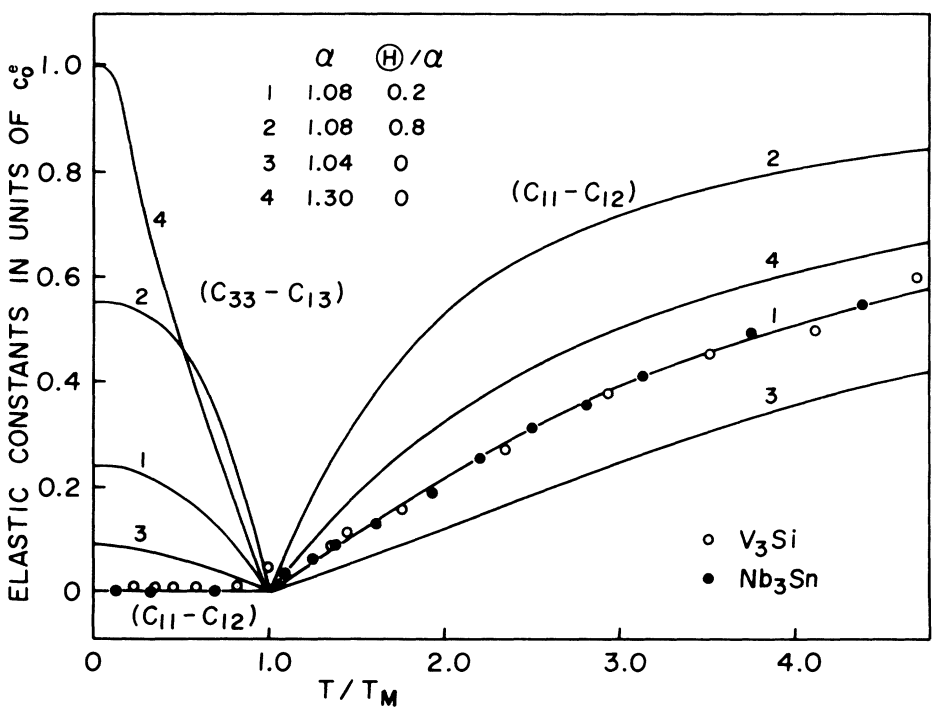

FIG. 7. Temperature dependence of the elastic constants. The solid lines are the calculations for some values of α and Θ. The line 4 corresponds to the case of the first-order Jahn-Teller effect. The calculated $c_{11}-c_{12}$ vanishes below T_M. The experimental data of $c_{11}-c_{12}$ on V_3Si (Ref. 10) and Nb_3Sn (Ref. 11) are also shown.

V. PHONON SOFTENING

We consider phonons with wave vector $\vec{q}$ of small magnitude, since the electrons in a small region containing the Γ point participate to the structural transition. The phonons at small q in the absence of the electron-lattice coupling are known by applying the idea of $\vec{k}\cdot\vec{p}$ perturbation theory to lattice dynamics.[39] All phonon normal modes at $\vec{q}=0$ mix with each other at a general $\vec{q}$ ($\neq 0$). In the following, however, we neglect the phonon modes other than the three acoustic and Γ_{12} optic modes, since they do not couple to the Γ_{12} electrons. At $\vec{q}=0$, the eigenvectors of the Γ_{12} optic modes, $\vec{e}_2$ and $\vec{e}_3$, are given by Eqs. (2) and (3), whereas those of the acoustic modes $s=4$, 5, and 6, $\vec{e}_4$, $\vec{e}_5$, and $\vec{e}_6$, correspond to the translations of the crystal as a whole along the x, y, and z axes. Their eigenvectors at $\vec{q}\neq 0$, $\vec{e}_s(\vec{q})$, are expressed as

$$\vec{e}_s(\vec{q})=\sum_{s'} U^p_{ss'}(\vec{q})\vec{e}_{s'} . \tag{25}$$

The phonon frequency $\omega_{\vec{q}s}$ together with $U^p_{ss'}(\vec{q})$ satisfies

$$\sum_{s'} D_{ss'}(\vec{q})U^p_{s''s'}(\vec{q})=\omega^2_{\vec{q}s''}U^p_{s''s}(\vec{q}) , \tag{26}$$

where $D_{ss'}(\vec{q})$ is an element of the dynamical matrix $\underline{D}(\vec{q})$. We expand $\underline{D}(\vec{q})$ in powers of $\vec{q}$ and use a symmetry consideration to obtain $\underline{D}(\vec{q})$. The obtained result is given by Eq. (27) where m_d is the density of mass, c^0_{11}, c^0_{12}, and c^0_{44} are the elastic constants in the absence of the Γ_{12} subbands and the Γ_{12} optic modes, and c_i and c_i' are some expansion coefficients,

$$\underline{D}(\vec{q})=\begin{bmatrix}
\omega_i^2+c_iq^2+\frac{c_i'}{\sqrt{6}}(3q_z^2-q^2) & \frac{c_i'}{\sqrt{2}}(q_x^2-q_y^2) & \frac{i\zeta}{\sqrt{2}}\left[\frac{c_0}{m_d}\right]^{1/2}\omega_iq_x & -\frac{i\zeta}{\sqrt{2}}\left[\frac{c_0}{m_d}\right]^{1/2}\omega_iq_y & 0 \\
\frac{c_i'}{\sqrt{2}}(q_x^2-q_y^2) & \omega_i^2+c_iq^2-\frac{c_i'}{\sqrt{6}}(3q_z^2-q^2) & -\frac{i\zeta}{\sqrt{6}}\left[\frac{c_0}{m_d}\right]^{1/2}\omega_iq_x & -\frac{i\zeta}{\sqrt{6}}\left[\frac{c_0}{m_d}\right]^{1/2}\omega_iq_y & \frac{2i\zeta}{\sqrt{6}}\left[\frac{c_0}{m_d}\right]^{1/2}\omega_iq_z \\
-\frac{i\zeta}{\sqrt{2}}\left[\frac{c_0}{m_d}\right]^{1/2}\omega_iq_x & \frac{i\zeta}{\sqrt{6}}\left[\frac{c_0}{m_d}\right]^{1/2}\omega_iq_x & \frac{c^0_{11}}{m_d}q_x^2+\frac{c^0_{44}}{m_d}(q_y^2+q_z^2) & \frac{c^0_{12}+c^0_{44}}{m_d}q_xq_y & \frac{c^0_{12}+c^0_{44}}{m_d}q_xq_z \\
\frac{i\zeta}{\sqrt{2}}\left[\frac{c_0}{m_d}\right]^{1/2}\omega_iq_y & \frac{i\zeta}{\sqrt{6}}\left[\frac{c_0}{m_d}\right]^{1/2}\omega_iq_y & \frac{c^0_{12}+c^0_{44}}{m_d}q_yq_x & \frac{c^0_{11}}{m_d}q_y^2+\frac{c^0_{44}}{m_d}(q_z^2+q_x^2) & \frac{c^0_{12}+c^0_{44}}{m_d}q_yq_z \\
0 & -\frac{2i\zeta}{\sqrt{6}}\left[\frac{c_0}{m_d}\right]^{1/2}\omega_iq_z & \frac{c^0_{12}+c^0_{44}}{m_d}q_zq_x & \frac{c^0_{12}+c^0_{44}}{m_d}q_zq_y & \frac{c^0_{11}}{m_d}q_z^2+\frac{c^0_{44}}{m_d}(q_x^2+q_y^2)
\end{bmatrix} . \tag{27}$$

In obtaining Eq. (27), we already took into account that the potential energies for some ionic displacements with $\vec{q}=0$ are expressed as in Eq. (11). In terms of the phonons obtained by solving Eqs. (25)–(27), we write the Hamiltonian of the electron-phonon system as follows:

$$H=\sum_{\vec{k},\nu}\epsilon_{\vec{k}\nu}a^\dagger_{\vec{k}\nu}a_{\vec{k}\nu}+\sum_{\vec{q},s}\hbar\omega_{\vec{q}s}b^\dagger_{\vec{q}s}b_{\vec{q}s}+\sum_{\vec{q},s}\sum_{\nu,\nu'}\left[\frac{\hbar\omega_{\vec{q}s}}{2N}\right]^{1/2}g_{\vec{q}s,\nu\nu'}\rho_{-\vec{q},\nu\nu'}\phi_{\vec{q}s} , \tag{28}$$

with

$$\rho_{-\vec{q},\nu\nu'}=\sum_{\vec{k}}a^\dagger_{\vec{k}+\vec{q},\nu}a_{\vec{k}\nu'} ,$$

$$\phi_{\vec{q}s}=(b_{\vec{q}s}+b^\dagger_{-\vec{q}s}) ,$$

where $b_{\vec{q}s}$ and $b^\dagger_{\vec{q}s}$ are the phonon annihilation and creation operators, respectively. The electron-phonon coupling constants $g_{\vec{q}s,\nu\nu'}$ in Eq. (28) are related to each other through the crystal symmetry.[23] As will be shown in Appendix B, they have the following form:

$$\begin{aligned}
g_{\vec{q}s,\nu\nu'}=\frac{1}{\omega_{\vec{q}s}}\Bigg\{&\left[\omega_ig_iU^p_{s2}(\vec{q})+i\left[\frac{c_0}{2m_d}\right]^{1/2}g_0[q_xU^p_{s4}(\vec{q})-q_yU^p_{s5}(\vec{q})]\right](\delta_{\nu2}\delta_{\nu'3}+\delta_{\nu3}\delta_{\nu'2}) \\
&+\left[\omega_ig_iU^p_{s3}(\vec{q})+i\left[\frac{c_0}{6m_d}\right]^{1/2}g_0[2q_zU^p_{s6}(\vec{q})-q_xU^p_{s4}(\vec{q})-q_yU^p_{s5}(\vec{q})]\right](\delta_{\nu2}\delta_{\nu'2}-\delta_{\nu3}\delta_{\nu'3}) \\
&+\left[i\left[\frac{c_0}{3m_d}\right]^{1/2}g_0'[q_xU^p_{s4}(\vec{q})+q_yU^p_{s5}(\vec{q})+q_zU^p_{s6}(\vec{q})]\right](\delta_{\nu2}\delta_{\nu'2}+\delta_{\nu3}\delta_{\nu'3})\Bigg\} ,
\end{aligned} \tag{29}$$

where g_0' is a constant and $\delta_{\nu\nu'}$ is the Kronecker δ function. The term in g_0' in Eq. (29) arises from the coupling between the electrons and the Γ_1 mode of distortion which was not taken into account in Eq. (5).

Sham,[23] Bhatt and McMillan,[25] and Bhatt and Lee[40] studied the lattice dynamics for the model with the three one-dimensional bands (Labbé and Friedel model) and the Gor'kov model by using their respective methods. Here we investigate the resonant frequencies of the Γ_{12}-subband electron-phonon system on the basis of the linear-response theory.[41] The thermal average of the electron density varying with space $\vec{r}$ and time t,

$$\langle \rho_{\vec{q},\nu\nu'} \rangle_\Omega \exp(i\vec{q}\cdot\vec{r} - i\Omega t + \delta t) , \quad \delta = 0^+$$

induce those of the phonons

$$\langle \phi_{\vec{q}s} \rangle_\Omega \exp(i\vec{q}\cdot\vec{r} - i\Omega t + \delta t)$$

and vice versa through the electron-phonon coupling. When the retarded Green's function of free phonon $D_s^R(\vec{q},\Omega)$ and that of free electron $G_{\nu\nu'}^R(\vec{q},\Omega)$ are defined, as usual, by

$$D_s^R(\vec{q},\Omega) = \frac{2\hbar\omega_{\vec{q}s}}{(\hbar\Omega + i\delta)^2 - (\hbar\omega_{\vec{q}s})^2} \tag{30}$$

and

$$G_{\nu\nu'}^R(\vec{q},\Omega) = 2\sum_{\vec{k}} \left[\frac{f_\nu(\epsilon_{\vec{k}+\vec{q}}) - f_{\nu'}(\epsilon_{\vec{k}})}{\epsilon_{\vec{k}+\vec{q},\nu} - \epsilon_{\vec{k}\nu'} + \hbar\Omega + i\delta} \right] , \tag{31}$$

$\langle \rho_{\vec{q},\nu\nu'} \rangle_\Omega$ and $\langle \phi_{\vec{q}s} \rangle_\Omega$ should satisfy the self-consistent equations as follows:

$$\langle \phi_{\vec{q}s} \rangle_\Omega - \sum_{\nu,\nu'} \left[\frac{\hbar\omega_{\vec{q}s}}{2N} \right]^{1/2} g^*_{\vec{q}s,\nu\nu'} \times D_s^R(\vec{q},\Omega) \langle \rho_{\vec{q},\nu\nu'} \rangle_\Omega = 0 , \tag{32}$$

$$\langle \rho_{\vec{q},\nu\nu'} \rangle_\Omega - \sum_s \left[\frac{\hbar\omega_{\vec{q}s}}{2N} \right]^{1/2} g_{\vec{q}s,\nu\nu'} \times G_{\nu\nu'}^R(\vec{q},\Omega) \langle \phi_{\vec{q}s} \rangle_\Omega = 0 . \tag{33}$$

The resonant phonon frequencies Ω are determined from the condition that Eqs. (32) and (33) have a nontrivial solution of $\langle \phi_{\vec{q}s} \rangle_\Omega$ and $\langle \rho_{\vec{q},\nu\nu'} \rangle_\Omega$, i.e.,

$$| \underline{\Lambda}(\vec{q},\Omega) - \Omega^2 \underline{I} | = 0 , \tag{34}$$

where $\underline{I}$ is the 5×5 unit matrix and $\underline{\Lambda}(\vec{q})$ is the 5×5 matrix defined by

$$\Lambda_{ss'}(\vec{q},\Omega) = \omega_{\vec{q}s}\omega_{\vec{q}s'} \left[\delta_{ss'} + N^{-1} \sum_{\nu,\nu'} g^*_{\vec{q}s,\nu\nu'} g_{\vec{q}s',\nu\nu'} \times G_{\nu\nu'}^R(\vec{q},\Omega) \right] . \tag{35}$$

As seen from Eqs. (34) and (35), the phonons in the absence of the electron-lattice coupling interact on each other via electrons. The three of the solutions of Eq. (34) give new acoustic modes whose frequencies are zero at $\vec{q}=0$. In the $A15$ compounds, the tetragonal distortion u_3 and the optic-mode displacement Q_3 appear below T_M. The soft modes of these compounds are, therefore, one of such acoustic modes. We discuss mainly the acoustic modes in order to clarify a relation between the phonon softening and the phase transition. For these modes, $G_{\nu\nu'}^R(\vec{q},\Omega)$ in Eq. (35) are approximated by $\mathrm{Re}G_{\nu\nu'}^R(\vec{q},0)$, where Re means the real part of quantities. Since $g_{\vec{q}s,\nu\nu'}$ given by Eq. (29) is strongly anisotropic with respect to the direction of $\vec{q}$, the softening also depends on the direction of $\vec{q}$.[40,42] We substitute Eq. (29) with $\omega_{\vec{q}s}$ and $U_{ss'}^p(\vec{q})$ which are known from Eqs. (26) and (27) into Eq. (35), and solve Eq. (34) approximately. The obtained acoustic phonon frequencies are as follows: When $\vec{q}=(q/\sqrt{2},q/\sqrt{2},0)$,

$$\Omega^2_{\vec{q},[110]\mathrm{T}_1} = \frac{c_0^e}{2m_d} q^2 \left[\frac{1 + N^{-1}G_0^2 \mathrm{Re}[G_{23}^R(\vec{q},0) + G_{32}^R(\vec{q},0)]}{1 + N^{-1}g_i^2 \mathrm{Re}[G_{23}^R(\vec{q},0) + G_{32}^R(\vec{q},0)]} \right] , \tag{36}$$

$$\begin{aligned}\Omega^2_{\vec{q},[110]\mathrm{L}} = \frac{q^2}{2m_d} (& (c_{11}^0 + c_{12}^0 + 2c_{44}^0 - \tfrac{1}{3}\zeta^2 c_0) + \tfrac{1}{3}c_0 \{ 1 + N^{-1}g_i^2 \mathrm{Re}[G_{22}^R(\vec{q},0) + G_{33}^R(\vec{q},0)] \}^{-1} \\ & \times [(g_0 - \sqrt{2}g_0' - \zeta g_i)^2 N^{-1} \mathrm{Re}G_{22}^R(\vec{q},0) + (g_0 + \sqrt{2}g_0' - \zeta g_i)^2 N^{-1} \mathrm{Re}G_{33}^R(\vec{q},0) \\ & + 8g_0'^2 g_i^2 N^{-2} \mathrm{Re}G_{22}^R(\vec{q},0) \mathrm{Re}G_{33}^R(\vec{q},0)]) ,\end{aligned} \tag{37}$$

$$\Omega^2_{\vec{q},[110]T_2}=(c^0_{44}/m_d)q^2 , \tag{38}$$

and when $\vec{q}=(0,0,q)$,

$$\Omega^2_{\vec{q},[001]L}=\frac{q^2}{m_d}\Big((c^0_{11}-\tfrac{2}{3}\zeta^2 c_0)+\tfrac{2}{3}c_0\{1+N^{-1}g_i^2\mathrm{Re}[G^R_{22}(\vec{q},0)+G^R_{33}(\vec{q},0)]\}^{-1}$$
$$\times[(g_0+g_0'/\sqrt{2}-\zeta g_i)^2N^{-1}\mathrm{Re}G^R_{22}(\vec{q},0)+(g_0-g_0'/\sqrt{2}-\zeta g_i)^2N^{-1}\mathrm{Re}G^R_{33}(\vec{q},0)$$
$$+2g_0'^2g_i^2N^{-2}\mathrm{Re}G^R_{22}(\vec{q},0)\mathrm{Re}G^R_{33}(\vec{q},0)]\Big) , \tag{39}$$

$$\Omega^2_{\vec{q},[001]T_1}=\Omega^2_{\vec{q},[001]T_2}=(c^0_{44}/m_d)q^2 . \tag{40}$$

In Eqs. (36)–(40), we have specified the modes $s=4$, 5, and 6 in terms of the direction of $\vec{q}$ and the polarization; the polarization vector of $[110]T_1$ is parallel to $[1\bar{1}0]$. By using Eqs. (31) and (36), $\Omega^2_{\vec{q},[110]T_1}$ is rewritten more explicitly as

$$\Omega^2_{\vec{q},[110]T_1}=\frac{c_0^e}{2m_d}\left[\frac{1-\alpha\chi(T,q)}{1-\Theta\chi(T,q)}\right]q^2 , \tag{41}$$

with

$$\chi(T,q)=\frac{1}{2qk_F}\sum_{\nu=2}^{3}\int_0^\infty \frac{k}{1+\exp[(\hbar^2k^2/2m^*+(-1)^\nu\sqrt{C_0V/N}\,G_0u-\mu)/k_BT]}$$
$$\times\ln\left|\frac{(\hbar^2/2m^*)(2kq+q^2)-2(-1)^\nu\sqrt{C_0V/N}\,G_0u}{(\hbar^2/2m^*)(-2kq+q^2)-2(-1)^\nu\sqrt{C_0V/N}\,G_0u}\right|dk , \tag{42}$$

where $\hbar k_F$ is the Fermi momentum in the undistorted crystal. Expanding $\chi(T,q)$ in powers of q, and using Eqs. (23) and (41), we can show that the sound velocity $\lim_{q\to 0}(\Omega_{\vec{q},[110]T_1}/q)$ vanishes at $T=T_M$, and the $[110]T_1$ mode is the soft mode. However, $\lim_{q\to 0}(\Omega_{\vec{q},[110]T_1}/q)$ vanishes also at $T<T_M$ because of the presence of the equilibrium conditions (14) and (15). This is again characteristic of the Γ_{12}-subband model.

Figure 8 shows the acoustic-phonon frequencies at $T=0$ and ∞ which are obtained for a set of the values of the parameters in Eqs. (36)–(40). The modes $[110]T_2$, $[001]T_1$, and $[001]T_2$ are unchanged by the phase transition, since these modes do not couple to the Γ_{12}-subband electrons. The mode $[110]T_1$ is remarkably softened, especially in a region of $0<q\lesssim 2k_F$, while the softenings of [110]L and [001]L are smaller than that of $[110]T_1$. This difference originates mainly from the fact that local distortions produced by [110]L and [001]L with small q contain small tetragonal- and orthorhombic-type distortions compared to those produced by $[110]T_1$. Some of these properties of the acoustic phonons were also obtained for the Gor'kov model by Bhatt and McMillan.[25] Our softenings of the acoustic phonons agree qualitatively with the observations on V_3Si above T_M.[12] From Eq. (41) we see that $\Omega_{\vec{q},[110]T_1}$ is characterized by α and Θ. Fig-

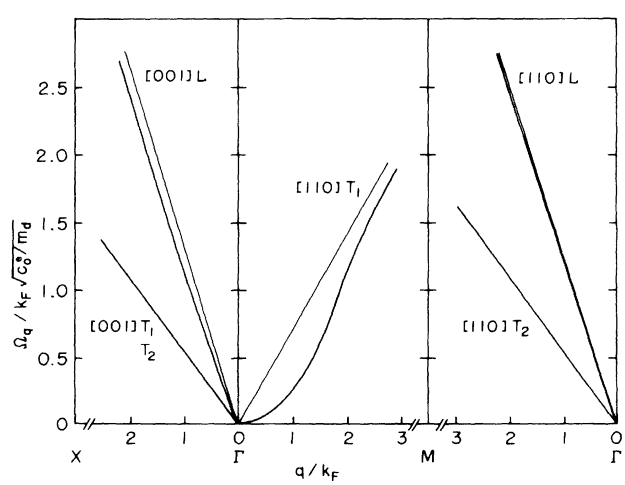

FIG. 8. Calculated dispersion curves of the acoustic phonons along some directions of wave vector $\vec{q}$. The bold and thin lines correspond to $T=0$ and ∞, respectively. The lines were depicted as an example for a set of the values as $\alpha=1.08$, $\Theta=0.22$, $\zeta=g_0'=0$, $c^0_{11}/c_0=1.8$, $c^0_{12}/c_0=0.8$, and $c^0_{44}/c_0=0.3$.

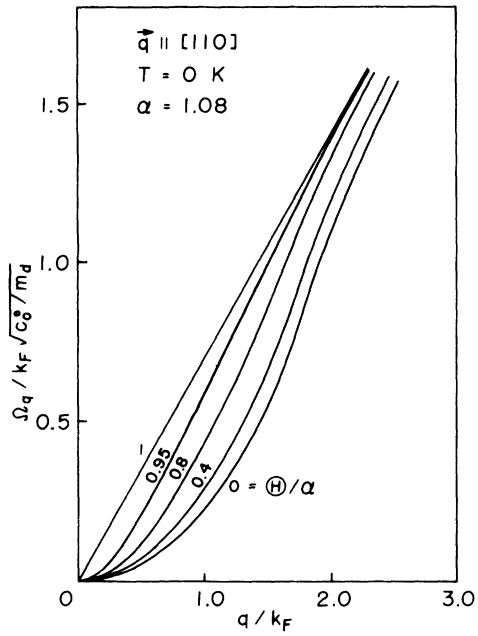

FIG. 9. Θ dependence of the dispersion curve of the $[110]T_1$ mode ($\vec{q}||[110]$, $\vec{e}||[1\bar{1}0]$) at zero temperature. The sound velocity at the limit $q\rightarrow 0$ is always zero except for $\Theta/\alpha=1$.

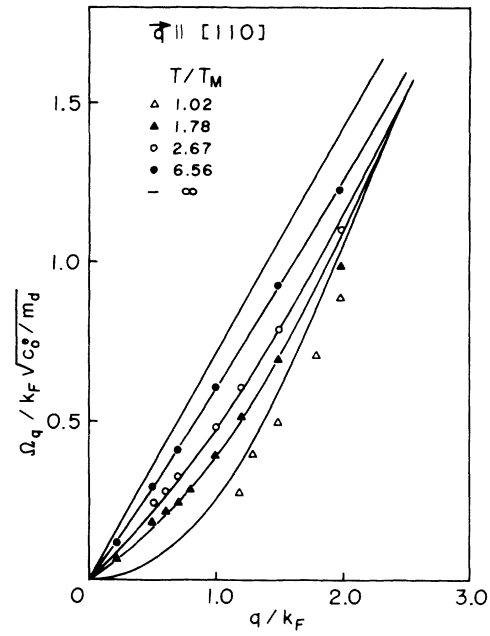

FIG. 10. Temperature dependence of the dispersion curve of the $[110]T_1$ mode ($\vec{q}||[110]$, $\vec{e}||[1\bar{1}0]$). The solid lines are the calculations at the temperatures given in the figure for $\alpha=1.08$ and $\Theta=0.22$. The experimental data on Nb_3Sn (Ref. 13) are also shown.

ure 9 shows the Θ dependence of $\Omega_{\vec{q},[110]T_1}$ at zero temperature for a fixed value of α. The softening of $\Omega_{\vec{q},[110]T_1}$ decreases with increasing Θ/α and disappears at $\Theta=\alpha$, although the sound velocity of $\Omega_{\vec{q},[110]T_1}$ at the limit $q\rightarrow 0$ is always zero except for $\Theta=\alpha$. We obtain $\Omega_{\vec{q},[110]T_1}$ above T_M by substituting $u=0$ and μ determined by Eq. (15) into Eqs. (41) and (42). The temperature dependence of $\Omega_{\vec{q},[110]T_1}$ thus obtained is shown in Fig. 10, and is compared to the experimental data on Nb_3Sn.[13] As seen from Fig. 10, the calculated sound velocity at $T>T_M$ is no longer zero. At temperatures near T_M, $d\Omega_{\vec{q},[110]T_1}/q$ changes significantly at $q\simeq k_F$. By comparing the calculated dispersion curves to the observed ones, k_F is determined to be about $0.28(\pi/a_0)$. The remaining parameters α and Θ are determined so that the temperature dependences of $\Omega_{\vec{q},[110]T_1}$ and $c_{11}-c_{12}$ above T_M are fitted to the experimental data. The obtained result is $\alpha=1.08$ and $\Theta=0.22$. The agreement between the theory and the experiments is satisfactory.[43] However, the calculated curves deviate from the experimental data at $q\gtrsim 2k_F$. This is because the Γ_{12} subbands used here do not reproduce the true subbands at large k and because the q dependence of the coupling between the acoustic phonons and the Γ_{12}-subband electrons cannot be neglected at large q. The observed softening of $\Omega_{\vec{q},[110]T_1}$ at $T\simeq T_M$ is a little larger than the calculated one. This seems to be due to the neglect of phonon damping in our calculation. According to neutron scattering experiments on Nb_3Sn, the broadening of the $[110]T_1$ phonon line increases rapidly below 60 K. Even at 5 K, which is sufficiently lower than T_M, the $[110]T_1$ mode has a large damping. These facts suggest that damping processes also play a role in the electron-phonon coupled modes.

Equation (34) gives also the optic-phonon frequencies $\Omega_{\vec{q}2}$ and $\Omega_{\vec{q}3}$. The matrix elements of $\underline{\Lambda}(\vec{q},\Omega)$ between the optic and acoustic modes become zero with decreasing q to zero. The acoustic modes modify the dispersion of $\Omega_{\vec{q}2}$ and $\Omega_{\vec{q}3}$ by only a little amount at small q being neglected. Then $\Omega_{\vec{q}2}$ and $\Omega_{\vec{q}3}$ satisfy the approximate equations as

$$\Omega^2_{\vec{q}2}=\omega_i^2\{1+N^{-1}g_i^2\mathrm{Re}[G^R_{23}(\vec{q},\Omega_{\vec{q}2})+G^R_{32}(\vec{q},\Omega_{\vec{q}2})]\}\ , \quad (43)$$

$$\Omega^2_{\vec{q}3}=\omega_i^2\{1+N^{-1}g_i^2\mathrm{Re}[G^R_{22}(\vec{q},\Omega_{\vec{q}3})+G^R_{33}(\vec{q},\Omega_{\vec{q}3})]\}\ . \quad (44)$$

When $g_0=\zeta=0$, i.e., the acoustic modes do not at all participate to the structural transition, and moreover, when g_i^2 is sufficiently large, Eqs. (43) and (44)

give the solution $\Omega_{\vec{q}2},\Omega_{\vec{q}3}\propto q$ which can be the soft-mode frequencies. When g_0 and/or $\zeta\neq 0$ as in V_3Si and Nb_3Sn, G_0^2 is greater than g_i^2. The $[110]T_1$ mode, therefore, becomes unstable at the highest temperature giving T_M, as seen from Eqs. (36), (43), and (44). In this case Ω_{02} and Ω_{03} are not affected by the structural transition since $G^R_{\nu\nu'}(0,\Omega_{0\nu'})$ vanishes for $\Omega_{0\nu'}\neq 0$.[23] This is the reason why the observed Raman shift of the Γ_{12} optic phonons in V_3Si exhibits only a weak temperature dependence in the cubic phase.[15]

VI. CONCLUDING REMARKS

The various aspects of the structural phase transition in the $A15$ compounds have been explained successfully by ascribing the phase transition to the Γ_{12}-subband electrons near the Fermi level. It has been shown that the observed peculiar properties such as the weak first-order structural phase transition, the stabilities of $c/a>1$ and $c/a<1$ being almost the same, and $c_{11}-c_{12}\simeq 0$ in the tetragonal phase originate from the properties of the coupling between the Γ_{12}-subband electrons and the lattice. We approximated the Γ_{12} subbands by the two parabolic bands. This approximation is justified only in a small region containing the Γ point. The bands other than the Γ_{12} subbands were not treated explicitly. Those bands are insensitive to the structural change, but behave as an electron reservoir for the Γ_{12} subbands. Moreover, we neglected the Coulomb interactions between electrons, which reduce the band electron-lattice coupling through the screening process. These approximations must be improved for more quantitative studies on the structural phase transition.

Here we compare our theory to the earlier works on the structural transition in the $A15$ compounds. Labbé and Friedel[16] and other authors[24,44,45] assumed threefold-degenerate bands for the bands causing the structural instability. The ground electronic state in the tetragonal phase is a singlet or doublet depending on the sign of $c/a-1$. This means that the electronic free energy is not an even function of $c/a-1$ even in the absence of the higher-order couplings between the electron and the lattice, and gives the first-order phase transition. This situation holds also for the $R(4)$ model proposed by Lee, Birman, and Williamson.[46] In the case of the Γ_{12}-subband model, one of the two bands goes down while the other goes up, irrespective of the sign of $c/a-1$. Therefore the electronic free energy (except for the energy of the higher-order coupling) is symmetric with respect to the sign of $c/a-1$. The transition is almost of the second order if the third-order term in $c/a-1$, F_3, is sufficiently small. When F_3 becomes large, the discontinuous change of $c/a-1$ at T_M becomes large. Then the models of the twofold- and threefold-degenerate bands give similar properties of the structural phase transition. However, many experiments prove that F_3 is anomalously small in the $A15$ compounds. Another characteristic of the Γ_{12}-subband model is the isotropic nature in the u_2-u_3 plane. In the threefold-degenerate-band models, one of the two tetragonal distortions $c>a$ and $c<a$ is stabilized, depending on the electron number.[16] This means that the electronic free energy is strongly anisotropic in the u_2-u_3 plane. Also, in the Gor'kov model, there exists the anisotropy which originates from the anisotropic coupling between the electrons and the lattice. These strong anisotropies are unfavorable to the experimental facts such as $c_{11}-c_{12}\simeq 0$ below T_M and the stabilities of $c>a$ and $c<a$ being almost the same. The earlier models often assumed low dimensionality in the electron bands. Labbé and Friedel supposed that the sharp peaks in the one-dimensional bands of the cation chains are important to the structural instability. Gor'kov *et al.* also assumed a small interchain transfer of electrons so that the Fermi surface has well-developed flat portions containing the X points. In contrast to these models, the Γ_{12} subbands considered here are rather isotropic around the Γ point. Although there exists no sharp peak in the density of states of our bands, the structural transition can occur when the Fermi level lies above the band bottoms and the electron-lattice coupling is large enough to split the degenerate bands by a considerable amount. The assumed one dimensionality gives rise to another question. In crystals with the purely one-dimensional bands, long-period ionic displacements with $q=2k_F$ can occur through the Peierls instability if k_F is not placed at the zone boundaries. Even if nonzero transfers of electrons between the cation chains partially smear the flat portions of the Fermi surface, large Kohn anomalies can be expected at $q=2k_F$ on the Γ-X lines.[23,40] Experimentally, such anomalies have not been observed. The Γ_{12}-subband model, on the other hand, does not exhibit any notable softening of phonons at $q=2k_F$ on the Γ-X lines, being in agreement with the observations.[12,14]

In this paper we have extended the theory of the cooperative Jahn-Teller effect in localized electron systems[30,37] to the case of the band-electron system. It has been proven that the band Jahn-Teller effect has some characteristic properties such as the second-order Jahn-Teller effect and the softening of the acoustic $[110]T_1$ phonon in a range of $0<q\lesssim 2k_F$. The band Jahn-Teller effect for twofold-degenerate bands was discussed by some authors in order to explain the cubic-to-tetragonal

transitions in $LaAg_xIn_{1-x}$ (Refs. 47 and 48), $La_{3-x}S_4$ (Ref. 49), and also the $A15$ compounds.[50,51] In these theories, the bands are assumed to have sharp peaks whose positions or widths are changed by the structural change. Recently, Weber and Mattheiss[27] confirmed by calculating the energy bands for tetragonal Nb_3Sn that the Γ_{12} subbands are split significantly by the tetragonal distortion as predicted by $\vec{k}\cdot\vec{p}$ perturbation theory.[4] In the present theory together with Ref. 4, however, it has been emphasized that just the symmetry of the Γ_{12} subspace governs the various aspects of the structural phase transition in the $A15$ compounds.

We have not discussed the relation between the structural phase transition and the superconductivity. If the electrons in the Γ_{12} subbands pertain also to the superconductivity, both phase transitions can strongly interfere with each other. The study on this problem is left for the future.

APPENDIX A

We obtain here the electronic contribution to F_3, F_3^e. The following calculation is a simple extension of the theory made in the localized electron system[30,37] to the case of the band-electron system. The electron-lattice coupling has also the second-order terms in the displacements, $H'_{\vec{k}}$, which are expected to be smaller than the first-order terms in Eq. (5). Taking account of the relation (12) which is approximately true for a small higher-order term, we write $H'_{\vec{k}}$ in terms of only u_2 and u_3 as

$$H'_{\vec{k}} = -\left[\frac{V}{NC_0}\right]^{1/2} G_0 B_3 [\, 2u_2u_3(a_2^\dagger a_3 + a_3^\dagger a_2) + (u_2^2 - u_3^2) \times (a_2^\dagger a_2 - a_3^\dagger a_3)] \,, \tag{A1}$$

with the coupling constant B_3. The total Hamiltonian $(H_{\vec{k}} + H'_{\vec{k}})$ has the eigenvalues as

$$\left.\begin{matrix}\epsilon_{\vec{k}2}\\ \epsilon_{\vec{k}3}\end{matrix}\right\} = \frac{\hbar^2 k^2}{2m^*} \pm \left[\frac{C_0 V}{N}\right]^{1/2} G_0 u \times \left[1 + \left[\frac{2B_3}{C_0}\right] u\cos(3\theta)\right]^{1/2} , \tag{A2}$$

where a small term has been neglected. We substitute Eq. (A2) into the free energy F given by Eq. (11) and expand F in powers of B_3. F_3^e is obtained to be

$$\frac{F_3^e}{V} = -\left[\frac{V}{NC_0}\right]^{1/2} G_0 B_3 u^2 \cos(3\theta) \times \int \mathscr{D}(\epsilon)[f_3(\epsilon) - f_2(\epsilon)]d\epsilon \,. \tag{A3}$$

Equations (14) and (A3) lead us to

$$\frac{F_3^e}{V} = -B_3 u^3 \cos(3\theta) \,. \tag{A4}$$

APPENDIX B

The couplings between the Γ_{12}-subband electrons and phonons at small q are obtained by use of a symmetry consideration. The electron potential at $\vec{r}$ produced by ionic displacements is written as

$$\delta V(\vec{r}) = \sum_{j,\kappa,i} v_{\kappa i}(\vec{r} - \vec{R}_j)\delta u_{\kappa i}(j,\vec{r}) \,, \tag{B1}$$

where $v_{\kappa i}(\vec{r} - \vec{R}_j)$ is the potential at $\vec{r}$ produced by the unit displacement of the κth ion in the jth cell at $\vec{R}_j$ along the i axis, and $\delta u_{\kappa i}(j,\vec{r})$ is the net displacement effective to an electron at $\vec{r}$. Since electrons are also displaced by the acoustic modes, $\delta u_{\kappa i}(j,\vec{r})$ is given by

$$\delta u_{\kappa i}(j,\vec{r}) = \frac{1}{\sqrt{N}} \sum_{\vec{q},s} \left[\frac{1}{\sqrt{m_\kappa}} \sum_{s'=2}^{3} U_{ss'}^p(\vec{q}) e_{\kappa i,s'} + \frac{i}{\sqrt{\bar{m}}} e^{i\vec{q}\cdot\vec{r}_\kappa} \sum_{s'=4}^{6} \sum_{i'} U_{ss'}^p(\vec{q})(q_i e_{i's'} + q_{i'} e_{is'} - q_i e_{is'} \delta_{ii'})(\vec{r} - \vec{R}_j - \vec{r}_\kappa)_{i'} \right] Q_{\vec{q}s} e^{i\vec{q}\cdot\vec{R}_j} \,, \tag{B2}$$

where $\vec{e}_4$, $\vec{e}_5$, and $\vec{e}_6$ are the unit vectors along the x, y, and z axes, respectively, $U_{ss'}^p(\vec{q})$ is defined by Eq. (25), $\vec{r}_\kappa$ denotes the position of the κth ion in a unit cell, and $\bar{m}$ is the mean value of m_κ. The Γ_{12}-subband states, on the other hand, are expressed as

$$\Psi_{\vec{k}\nu}(\vec{r})=\frac{1}{\sqrt{V}}\sum_{\nu} U^e_{\nu\nu}\phi_\nu(\vec{r})e^{i\vec{k}\cdot\vec{r}}\,, \tag{B3}$$

where $\phi_\nu(\vec{r})=\phi_\nu(\vec{r}-\vec{R}_j)$. Equations (B1)—(B3) give

$$\langle\Psi_{\vec{k}+\vec{q},\nu}|\,\delta V\,|\,\Psi_{\vec{k}\nu}\rangle=\sum_{\vec{q},s}\sum_{\nu',\nu''}Q_{\vec{q}s}U^e_{\nu\nu'}U^e_{\nu'\nu''}\left[\sum_{s'=2}^{3}U^p_{ss'}(\vec{q})A_{\nu'\nu'',s'}+\sum_{s'=4}^{6}\sum_{i,i'}iU^p_{ss'}(\vec{q})q_ie_{i's'}A_{\nu'\nu'',ii'}\right]. \tag{B4}$$

In Eq. (B4) we have defined $A_{\nu'\nu'',s'}$ and $A_{\nu'\nu'',ii'}$ by

$$A_{\nu'\nu'',s'}=\sum_{\vec{g},\vec{g}'}\sum_{\kappa,i}\left[\frac{N}{m_\kappa}\right]^{1/2}e_{\kappa i,s'}\phi^*_{\vec{g}+\vec{g}',\nu'}\phi_{\vec{g}',\nu''}v_{\vec{g},\kappa i}\,, \tag{B5}$$

$$A_{\nu'\nu'',ii'}=\sum_{\vec{g},\vec{g}'}\sum_{\kappa}\left[\frac{N}{\bar{m}}\right]^{1/2}(v_{\vec{g},\kappa ii'}+v_{\vec{g},\kappa i'i})\phi^*_{\vec{g}+\vec{g}'\nu'}\phi_{\vec{g}'\nu''}\,, \tag{B6}$$

with

$$\phi_{\vec{g}\nu}=a_0^{-3}\int\phi_\nu(\vec{r})e^{-i\vec{g}\cdot\vec{r}}d\vec{r}\,,$$

$$v_{\vec{g},\kappa i}=\int v_{\kappa i}(\vec{r})e^{-i\vec{g}\cdot\vec{r}}d\vec{r}\,,$$

$$v_{\vec{g},\kappa ii'}=\int v_{\kappa i}(\vec{r})(\vec{r}-\vec{r}_\kappa)_{i'}e^{-i\vec{g}\cdot\vec{r}}d\vec{r}\,,$$

where $\vec{g}$ and $\vec{g}'$ are the reciprocal-lattice vectors, and $v_{\vec{g},\kappa i}$ and $v_{\vec{g},\kappa ii'}$ have been used, respectively, for $v_{(\vec{g}+\vec{q}),\kappa i}$ and $v_{(\vec{g}+\vec{q}),\kappa ii'}$ with small q. We can prove that the quantities $A_{\nu'\nu'',s'}$ are transformed by the symmetry operations in space group $Pm\,3n$ as the bases of the representation $\Gamma_{12}\times\Gamma_{12}\times\Gamma_{12}$, while the quantities $A_{\nu'\nu'',ii'}$ are transformed as those of $\Gamma_{12}\times\Gamma_{12}\times[\Gamma_{15}\times\Gamma_{15}]$. The nonvanishing quantities $A_{\nu'\nu'',s'}$ or $A_{\nu'\nu'',ii'}$ are found by using the fact that among the linear combinations between the quantities $A_{\nu'\nu'',s'}$ or $A_{\nu'\nu'',ii'}$ only the bases of the identity representations are nonvanishing constants. After some manipulations, Eq. (B4) is reduced to

$$\begin{aligned}\langle\Psi_{\vec{k}+\vec{q},\nu}|\,\delta V\,|\,\Psi_{\vec{k}\nu'}\rangle&=\sum_{\vec{q},s}\frac{Q_{\vec{q}s}}{\sqrt{N}}(\omega_ig_i[(U^e_{\nu2}U^e_{\nu'3}+U^e_{\nu3}U^e_{\nu'2})U^p_{s2}(\vec{q})+(U^e_{\nu2}U^e_{\nu'2}-U^e_{\nu3}U^e_{\nu'3})U^p_{s3}(\vec{q})]\\&\quad+i\left[\frac{c_0}{m_d}\right]^{1/2}g_0\{(U^e_{\nu2}U^e_{\nu'3}+U^e_{\nu3}U^e_{\nu'2})[q_xU^p_{s4}(\vec{q})-q_yU^p_{s5}(\vec{q})]/\sqrt{2}+(U^e_{\nu2}U^e_{\nu'2}-U^e_{\nu3}U^e_{\nu'3})\\&\qquad\times[2q_zU^p_{s6}(\vec{q})-q_xU^p_{s4}(\vec{q})-q_yU^p_{s5}(\vec{q})]/\sqrt{6}\}\\&\quad+i\left[\frac{c_0}{m_d}\right]^{1/2}g_0'\{(U^e_{\nu2}U^e_{\nu'2}+U^e_{\nu3}U^e_{\nu'3})[q_xU^p_{s4}(\vec{q})+q_yU^p_{s5}(\vec{q})+q_zU^p_{s6}(\vec{q})]/\sqrt{3}\})\,.\end{aligned} \tag{B7}$$

In obtaining Eq. (B7), we already took into account that Eq. (B7) with $\vec{q}=0$ should give the term of the coupling between the electrons and the displacements in Eq. (5). Replacing $U^e_{\nu\nu'}$ in Eq. (B7) by $\delta_{\nu\nu'}$ in the cubic and tetragonal phases, and comparing Eq. (B7) to Eq. (28), we arrive at Eq. (29).

[1]M. Weger and I. B. Goldberg, in *Solid State Physics,* edited by H. Ehrenreich, F. Seitz, and D. Turnbull (Academic, New York, 1973), Vol. 28, p. 1.
[2]Yu.A. Izyumov and Z. Z. Kurmaev, Usp. Fiz. Nauk. 113, 193 (1974) [Sov. Phys.—Usp. 17, 356 (1974)].
[3]L. R. Testardi, Rev. Mod. Phys. 47, 637 (1975).
[4]M. Kataoka, Phys. Lett. 80A, 35 (1980).
[5]B. W. Batterman and C. B. Barrett, Phys. Rev. 145, 296 (1966).
[6]R. Mailfert, B. W. Batterman, and J. J. Hanak, Phys. Lett. 24A, 315 (1967); Phys. Status Solidi 32, K67 (1969).
[7]G. Shirane and J. D. Axe, Phys. Rev. B 4, 2957 (1971).
[8]L. J. Vieland, J. Phys. Chem. Solids 31, 1449 (1970).
[9]Y. Fujii, J. B. Hastings, M. Kaplan, G. Shirane, Y. Inada, and N. Kitamura, Phys. Rev. B 25, 364 (1982).
[10]L. R. Testardi and T. B. Bateman, Phys. Rev. 154, 402 (1967).
[11]K. R. Keller and J. J. Hanak, Phys. Rev. 154, 628 (1967).
[12]G. Shirane, J. D. Axe, and R. J. Birgeneau, Solid State Commun. 9, 397 (1971).
[13]G. Shirane and J. D. Axe, Phys. Rev. Lett. 27, 1803 (1971).
[14]J. D. Axe and G. Shirane, Phys. Rev. B 8, 1965 (1973).
[15]H. Wipf, M. V. Klein, B. S. Chandrasekhar, T. H. Geballe, and J. H. Wernick, Phys. Rev. Lett. 41, 1752 (1978).
[16]P. J. Labbé and J. Friedel, J. Phys. (Paris) 27, 153 (1966); 27, 303 (1966).
[17]L. P. Gor'kov, Zh. Eksp. Teor. Fiz. 65, 1658 (1973) [Sov. Phys.—JETP 38, 830 (1974)].
[18]L. P. Gor'kov and O. N. Dorokhov, J. Low Temp. Phys. 22, 1 (1976).
[19]L. F. Mattheiss, Phys. Rev. 138, A112 (1965).
[20]B. M. Klein, L. L. Boyer, D. A. Papaconstantopoulos, and L. F. Mattheiss, Phys. Rev. B 18, 6411 (1978).
[21]W. E. Pickett, K. M. Ho, and M. L. Cohen, Phys. Rev. B 19, 1734 (1979).
[22]T. Jarlborg and G. Arbman, J. Phys. F 6, 189 (1976).
[23]L. J. Sham, Phys. Rev. Lett. 27, 1725 (1971); Phys. Rev. B 6, 3584 (1972).
[24]J. Noolandi and L. J. Sham, Phys. Rev. B 8, 2468 (1973).
[25]R. N. Bhatt and W. L. McMillan, Phys. Rev. B 14, 1007 (1976).
[26]L. F. Mattheiss and W. Weber, Phys. Rev. B 25, 2248 (1982).
[27]W. Weber and L. F. Mattheiss, Phys. Rev. B 25, 2270 (1982).
[28]G. L. Bir and G. E. Pikus, *Symmetry and Strain-Induced Effects in Semiconductors* (Wiley, New York, 1974), p. 295.
[29]M. Born and K. Huang, *Dynamical Theory of Crystal Lattices* (Clarendon, Oxford, 1968), p. 129.
[30]J. Kanamori, J. Appl. Phys. 31, 14S (1960).
[31]P. W. Anderson and E. I. Blount, Phys. Rev. Lett. 14, 217 (1965).
[32]B. S. Chandrasekhar, H. R. Ott, and B. Seeber, Solid State Commun. 39, 1265 (1981).
[33]L. J. Vieland, R. W. Cohen, and W. Rehwald, Phys. Rev. Lett. 26, 373 (1971).
[34]W. Rehwald, M. Rayl, R. W. Cohen, and G. D. Cody, Phys. Rev. B 6, 363 (1972).
[35]J. P. Maita and E. Bucher, Phys. Rev. Lett. 29, 931 (1972).
[36]The optic-mode displacement in the tetragonal phase is Q_3, which accords with the observed mode of the sublattice displacements.
[37]M. Kataoka and J. Kanamori, J. Phys. Soc. Jpn. 32, 113 (1972).
[38]Reference 34 also observed $c_{11}-c_{12}$ of Nb_3Sn, which did not show the softening at low temperatures, differing from the data obtained by Keller and Hanak (Ref. 11). The former group's data correspond to the elastic constants averaged over tetragonal domains below T_M. Since both groups detected no echo of the sound with the polarization vector parallel to $[1\bar{1}0]$ propagated along [110], we employed here the data in Ref. 11.
[39]*Solid State Theory—Methods and Applications,* edited by P. T. Landsberg (Wiley, New York, 1969), p. 366.
[40]R. N. Bhatt and P. A. Lee, Phys. Rev. B 16, 4288 (1977).
[41]A. L. Fetter and J. D. Walecka, *Quantum Theory of Many-Particle Systems* (McGraw-Hill, New York, 1971), p. 291.
[42]M. Kataoka and Y. Endoh, J. Phys. Soc. Jpn. 48, 912 (1980).
[43]The observed dispersion curve of the $[110]T_1$ mode of Nb_3Sn given in Ref. 14 is somewhat complicated and differs from that in Ref. 13. We employed here the latter which is consistent with our calculated results.
[44]R. W. Cohen, G. D. Cody, and J. J. Halloran, Phys. Rev. Lett. 19, 840 (1967).
[45]E. Pytte, Phys. Rev. Lett. 25, 1176 (1970).
[46]T. Lee, J. L. Birman, and S. J. Williamson, Phys. Rev. Lett. 39, 839 (1977); T. Lee and J. L. Birman, Phys. Rev. B 17, 4931 (1978).
[47]H. Ihrig, D. T. Vigren, J. Kübler, and S. Methfessel, Phys. Rev. B 8, 4525 (1973).
[48]S. K. Ghatak, D. K. Ray, and C. Tannous, Phys. Rev. B 18, 5379 (1978).
[49]D. K. Ray, K. Weterholt, S. Methfessel, and S. K. Ghatak, Solid State Commun. 38, 783 (1978).
[50]R. N. Bhatt, Phys. Rev. B 16, 1915 (1977).
[51]B. Pietrass, A. Handstein, and G. Behr, Phys. Status Solidi B 98, 597 (1980).